

# Supporting Material: Quantifying the rheological and hemodynamic characteristics of sickle cell anemia,

## by Lei and Karniadakis

### RBC membrane

In the equilibrium state, the RBC keeps a biconcave shape as described by Ref. (1). In the present model, the RBC membrane is represented by a two-dimensional triangulated network with  $N_v$  vertices where each vertex is represented by a DPD particle. The vertices are connected by  $N_s$  visco-elastic bonds to impose proper membrane mechanics (2, 3). Specifically, the elastic part of bond is represented by

$$V_s = \sum_{j \in 1 \dots N_s} \left[ \frac{k_B T l_m (3x_j^2 - 2x_j^3)}{4p(1-x_j)} + \frac{k_p}{(n-1)l_j^{n-1}} \right], \quad (\text{S1})$$

where  $l_j$  is the length of the spring  $j$ ,  $l_m$  is the maximum spring extension,  $x_j = l_j/l_m$ ,  $p$  is the persistence length,  $k_B T$  is the energy unit,  $k_p$  is the spring constant, and  $n$  is a power. Physically, the above two terms represent the wormlike chain potential and a repulsive potential, respectively.

The membrane viscosity is imposed by introducing a viscous force on each spring. Following the general framework of the fluid particle model (4), we can define the dissipative force  $\mathbf{F}_{ij}^D$  and random force  $\mathbf{F}_{ij}^R$  given by

$$\mathbf{F}_{ij}^D = -\gamma^T \mathbf{v}_{ij} - \gamma^C (\mathbf{v}_{ij} \cdot \mathbf{e}_{ij}) \mathbf{e}_{ij}, \quad (\text{S2})$$

$$\mathbf{F}_{ij}^R dt = \sqrt{2k_B T} \left( \sqrt{2\gamma^T} d\mathbf{W}_{ij}^S + \sqrt{3\gamma^C - \gamma^T} \frac{\text{tr}[d\mathbf{W}_{ij}]}{3} \mathbf{1} \right) \cdot \mathbf{e}_{ij}, \quad (\text{S3})$$

where  $\gamma^T$  and  $\gamma^C$  are dissipative parameters,  $\mathbf{v}_{ij}$  is the relative velocity of spring ends,  $\text{tr}[d\mathbf{W}_{ij}]$  is the trace of a random matrix of independent Wiener increments  $d\mathbf{W}_{ij}$ , and  $d\mathbf{W}_{ij}^S = d\mathbf{W}_{ij} - \text{tr}[d\mathbf{W}_{ij}]\mathbf{1}/3$  is the traceless symmetric part.

To uniquely relate the model parameters and visco-elastic properties of the cell membrane, we extend the linear analysis of (5) for a regular hexagonal network (3); the derived shear modulus of the membrane  $\mu_0$  is given by

$$\mu_0 = \frac{\sqrt{3}k_B T}{4pl_m x_0} \left( \frac{x_0}{2(1-x_0)^3} - \frac{1}{4(1-x_0)^2} + \frac{1}{4} \right) + \frac{\sqrt{3}k_p(n+1)}{4l_0^{n+1}}, \quad (\text{S4})$$

where  $l_0$  is the equilibrium spring length and  $x_0 = l_0/l_m$ . The membrane shear viscosity is given by  $\eta_m = \sqrt{3}\gamma^T + \gamma^C/4$ , where  $\gamma^T$  and  $\gamma^C$  are chosen such that the characteristic relaxation time of the present RBC model (mainly determined by the ratio of the membrane elastic and viscous force) matches the experimental measurements (6, 7).

The bending resistance of the RBC membrane is modeled by

$$V_b = \sum_{j \in 1 \dots N_s} k_b [1 - \cos(\theta_j - \theta_0)], \quad (\text{S5})$$

where  $k_b$  is the bending constant,  $\theta_j$  is the instantaneous angle between two adjacent triangles having the common edge  $j$ , and  $\theta_0$  is the spontaneous angle. The relation between the model bending coefficient  $k_b$

and the macroscopic bending rigidity  $k_c$  of the Helfrich model (8) can be derived as  $k_b = 2k_c/\sqrt{3}$  for a spherical membrane (3).

In addition, the RBC model includes the area and volume conservation constraints, which mimic the area-incompressibility of the lipid bilayer and the incompressibility of the interior fluid, respectively. The corresponding energy is given by

$$V_{a+v} = \sum_{j \in 1 \dots N_t} \frac{k_d(A_j - A_0)^2}{2A_0} + \frac{k_a(A - A_0^{tot})^2}{2A_0^{tot}} + \frac{k_v(V - V_0^{tot})^2}{2V_0^{tot}}, \quad (S6)$$

where  $N_t$  is the number of triangles in the membrane network,  $A_0$  is the triangle area, and  $k_d$ ,  $k_a$  and  $k_v$  are the local area, global area and volume constraint coefficients, respectively. The terms  $A$  and  $V$  are the total RBC area and volume, while  $A_0^{tot}$  and  $V_0^{tot}$  are the specified total area and volume, respectively. The corresponding area-compression  $K$  and Young's modulus  $Y$  are given by

$$K = 2\mu_0 + k_a + k_d, \quad Y = \frac{4K\mu_0}{K + \mu_0}. \quad (S7)$$

More details on the RBC model and the scaling between the model and the physical units can be found in Ref. (3).

## Construction of SS-RBC membrane

Different forces are applied at the anchor points on the cell membrane to mimic the various distortion effect on the cell membrane. The sickle and elongated cells originate from SS-RBCs with intracellular HbS polymer developing along a specific direction. The stretching force is applied on the anchor points "A" and "C" as shown in Fig. 1 in the manuscript. On the contrary, granular cells originated from SS-RBCs with intracellular HbS polymer domain with spherulitic configuration. Correspondingly, stretching forces are applied on all of the four anchor points shown in Fig. 1. The detail parameters for the stretching force for different shape of SS-RBC is shown in Tab. S1.

	A	B	C	D
S	(0.0, 55, 54)	(0.0, 0.0, 0.0)	(0.0, -55, 54)	(0.0, 0.0, 0.0)
G	(0.0, 23, 31)	(-23, 0.0, 31)	(0.0 - 23, 31)	(23, 0.0, 31)
E	(0, 55, 11)	(0, 0, 0)	(0, -55, -11)	(0, 0, 0)

Table S1: Stretching force (pN) applied on the anchor points for each type of the cell morphology.

## Adhesion model

During the simulation of present work, the adhesive bond formation and dissociation are executed in a stochastic way for each time step. First, all existing bonds between cell vertices and ligands are checked for a potential dissociation. A bond is ruptured if the bond length is larger than  $d_{off}$ , otherwise it is determined according to the probability  $P_{off}$ . Second, a bond formation procedure is looped through all the free ligands. For each free ligand, all the cell vertices within the distance  $d_{on}$  are examined, and bond formation is accepted in a stochastic way according to the probability  $P_{on}$ . Finally, the forces of all existing bonds are calculated and applied. Detail parameters for the adhesive interaction between the SS-RBC and ligands are shown in Tab. S2.

Parameters	Simulations	Physical
spring constant ( $k_s$ )	400	$1.85 \times 10^{-5} \text{ N/m}$
equilibrium spring length ( $l_0$ )	0.0	0.0 m
reactive distance ( $d_{on}$ )	0.5	$4.8 \times 10^{-7} \text{ m}$
rupture distance ( $d_{off}$ )	0.5	$4.8 \times 10^{-7} \text{ m}$
on strength ( $\sigma_{on}$ )	0.22	$1.02 \times 10^{-8} \text{ N/m}$
off strength ( $\sigma_{off}$ )	0.33	$1.52 \times 10^{-8} \text{ N/m}$
unstressed on rate ( $k_{on}^0$ )	600.0	$6.0 \times 10^5 \text{ s}^{-1}$
unstressed off rate ( $k_{off}^0$ )	0.25	$250 \text{ s}^{-1}$

Table S2: Simulation (in DPD units) and physical (in SI units) parameters for blood flow with adhesive interaction with vascular endothelium.

## Mathematical description of distorted RBC shapes

Sickle red blood cells (SS-RBC) undergo various morphological transitions in deoxygenated conditions. To quantify the distorted shape of SS-RBC, we use a polynomial function  $z = f(x, y)$  to fit the surface of the cell membrane for all the three types of cells, similar to the approach in Ref. (1). The polynomial function is defined by

$$f(x, y) = \alpha_0 + \alpha_1 x^2 + \alpha_2 y^2 + \alpha_3 x^4 + \alpha_4 y^4 + \alpha_5 x^2 y^2, \quad (\text{S8})$$

where  $\alpha_0, \alpha_1, \dots, \alpha_5$  are fitting coefficients determined by the specific shape of the cell and the boundary of the cell on the x-y plane is defined by

$$(x/b_1)^p + (y/b_2)^p = 1, \quad (\text{S9})$$

where  $b_1, b_2$  and  $p$  vary for different cell morphologies.

For each cell, the membrane is divided into two parts according to the dual values in z direction; each part is fitted by Eq. (S8) separately as shown in Figure S1. The combined surfaces define the cell membrane for the classical ‘‘sickle’’ shape of cell as shown in Figure S2. Similarly, the elongated and granular shape of cell membranes are fitted and plotted in Figure S3 and Figure S4.

We note that the basic morphological properties of the sickle cell can be interpreted from the fitting parameters used above. First,  $b_1$  and  $b_2$  defines the maximum extension along the x and y direction, which determines the length and width of the cells respectively. Second, the cell thickness can be quantified by the average value  $Z^T$  and the maximum extension  $Z^m$  along the z direction, both determined by the fitting parameter  $\alpha_0, \alpha_1, \dots, \alpha_5$ . Specifically, they are given by

$$\begin{aligned} Z^T &= \int (f^u(x, y) - f^l(x, y)) dS / S_0 \\ Z^m &= \max(f^u(x, y)) - \min(f^l(x, y)), \end{aligned} \quad (\text{S10})$$

where  $S_0$  is the surface area determined by Eq. (S9). Finally, the mean curvature  $C_H$  of the fitting surface is determined by  $\alpha_1, \dots, \alpha_5$  and given by

$$C_H(x, y) = \frac{\left(1 + \left(\frac{\partial f}{\partial x}\right)^2\right) \frac{\partial^2 f}{\partial y^2} - 2 \frac{\partial f}{\partial x} \frac{\partial f}{\partial y} \frac{\partial^2 f}{\partial x \partial y} + \left(1 + \left(\frac{\partial f}{\partial y}\right)^2\right) \frac{\partial^2 f}{\partial x^2}}{2 \left(1 + \left(\frac{\partial f}{\partial x}\right)^2 + \left(\frac{\partial f}{\partial y}\right)^2\right)^{3/2}}. \quad (\text{S11})$$

Analytical solution can be obtained as  $f(x, y)$  defined by the polynomial function.

Moreover, to quantify the difference between the fitting surface and the discrete cell vertices, we define the  $L_2$  error of the fitting normalized by the average thickness of SS-RBC, as

$$\epsilon = \frac{1}{N_v} \sqrt{\sum_{i=1}^{N_v} (f(x_i, y_i) - z_i)^2 / Z^T}, \quad (\text{S12})$$

where  $x_i, y_i$  and  $z_i$  are the coordinates of a discrete cell vertex,  $N_v$  is the total number of vertices considered.

The fitting parameters and the basic cell morphological properties (length, width, thickness, etc.) for each cell type are shown in Tab. S3 and Tab. S4.

## Movie Description

**Movie S1:** Blood flow of sickle cell in a straight tube with diameter  $D = 9\mu\text{m}$ , Hct = 30%. The shear modulus of the cell membrane is 100 times the value of healthy RBCs. Compared with blood plasma, the flow resistance increases about 50% due to the introduction of SS-RBCs. However, no blood occlusion is observed in the current work.

**Movie S2:** Blood flow of sickle cells with SS-RBC/wall adhesive interaction in a straight tube with diameter of  $D = 9\mu\text{m}$ . The green dots represent the ligands coated on the wall. The cells with blue color represent the “active” group of SS-RBCs exhibiting adhesive interaction with the coated ligands. The cells with red color represent the “non-active” group of cells. The shear modulus of both groups of cell is 100 times the value of healthy RBCs. The “active” cells show adhesion to channel wall in the region coated with ligands. Moreover, the adherent “active” cells may further trap the “non-active” cells, resulting in the flow occlusion in the channel.

	$\alpha_0$	$\alpha_1$	$\alpha_2$	$\alpha_3$	$\alpha_4$	$\alpha_5$	$\epsilon$
$S^l$	-0.806	-0.1141	$-6.78 \times 10^{-3}$	$2.12 \times 10^{-3}$	$2.01 \times 10^{-2}$	$2.84 \times 10^{-2}$	0.0748
$S^u$	1.36	-0.0403	0.306	$-1.69 \times 10^{-3}$	$-3.60 \times 10^{-2}$	$-2.77 \times 10^{-2}$	0.0748
$E^l$	-0.995	-0.0361	-0.092	$1.11 \times 10^{-3}$	$2.21 \times 10^{-2}$	$2.17 \times 10^{-2}$	0.0581
$E^u$	1.04	$8.36 \times 10^{-3}$	0.203	$-1.09 \times 10^{-3}$	$-2.89 \times 10^{-2}$	$-2.22 \times 10^{-2}$	0.0581
$G^l$	-0.237	-0.171	-0.180	$6.35 \times 10^{-3}$	$6.84 \times 10^{-3}$	$4.40 \times 10^{-2}$	0.0607
$G^u$	1.701	-0.0123	-0.0245	$-5.06 \times 10^{-3}$	$-4.86 \times 10^{-3}$	$-1.85 \times 10^{-2}$	0.0607

Table S3: The fitting parameters for the cell membranes with different morphologies. The label “S”, “E” and “G” represent the sickle, elongated and granular shape respectively. The upper label “u” and “l” represent the upper and lower part of the cell surface. The unit of  $x, y$  and  $z$  is in micrometer.

	$b_1$	$b_2$	$p$	$Z^T$	$Z^m$	$\langle C_H \rangle$
S	5.80	3.05	1.54	1.58	3.87	0.22
E	6.40	3.1	1.45	1.56	2.37	0.25
G	4.58	4.58	1.25	1.52	2.75	0.21

Table S4: The parameters of Eq. (S9) representing the boundary of cell on the x-y plane, where the surface of the cell membrane is defined. The label “S”, “E” and “G” represent the sickle, elongated and granular shape, respectively.  $Z^T$  and  $Z^m$  are the average/maximum cell thickness defined by Eq. (S10).  $\langle C_H \rangle$  is the average value of the mean curvature over the cell surface.

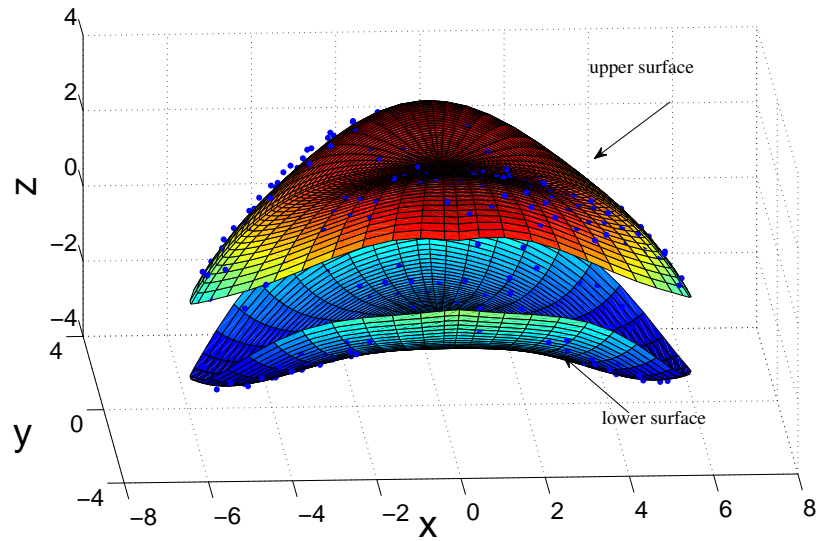


Figure S1: Fitted surface of cell membrane for the sickle shape of SS-RBC. For illustration purposes, the upper and lower surface is shifted by 1 and  $-1$  in the  $z$  direction respectively. The blue dots represent the cell vertices obtained from the procedure described in the current work. For details, see *Morphology of sickle red blood cell section* of the main text.

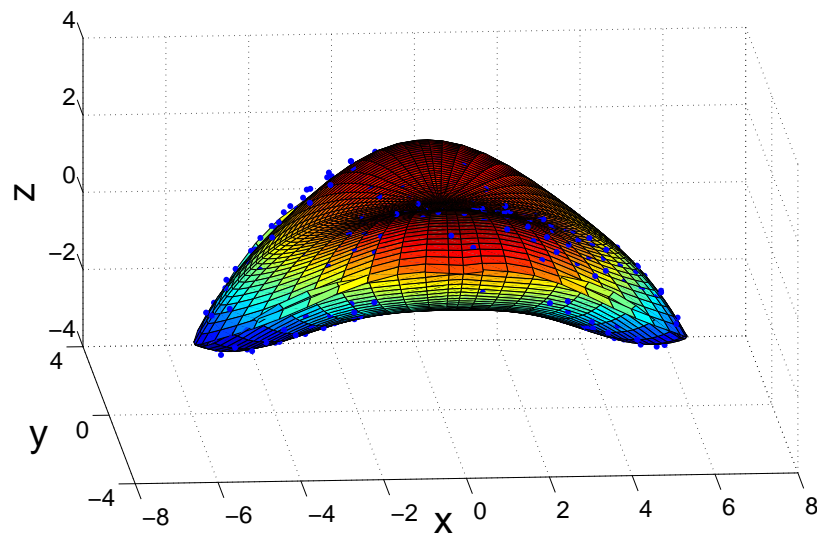


Figure S2: Cell vertices (blue dots) and the fitted surface of the cell membrane for the *sickle* shape of SS-RBC.

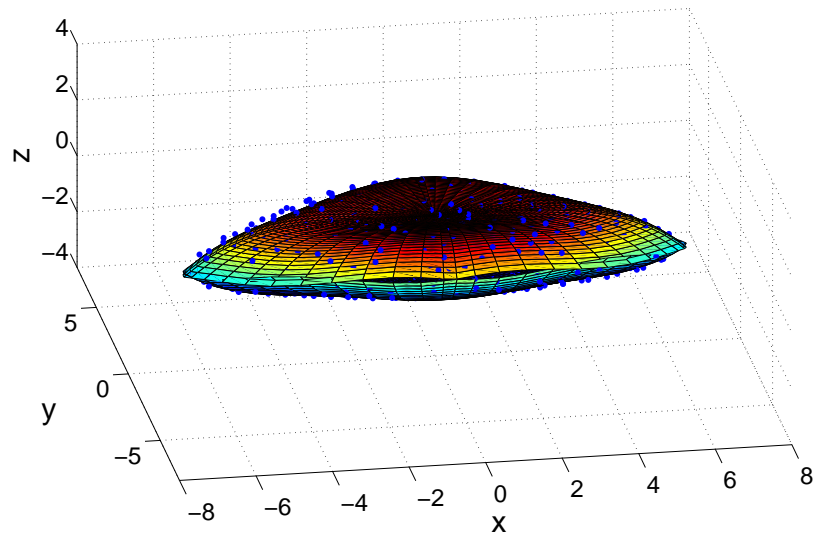


Figure S3: Cell vertices (blue dots) and the fitted surface of the cell membrane for the *elongated* shape of SS-RBC.

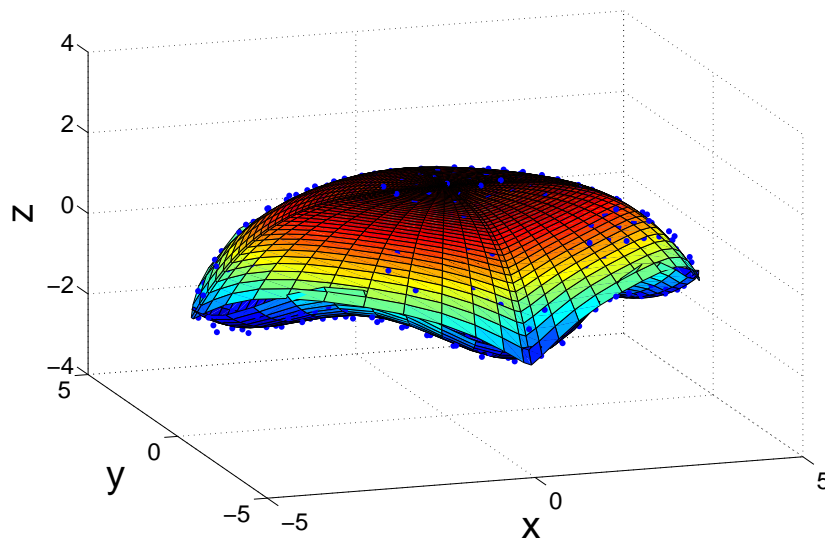


Figure S4: Cell vertices (blue dots) and the fitted surface of the cell membrane for the *granular* shape of SS-RBC.

## Supporting References

1. Evans, E. A., and R. Skalak, 1980. Mechanics and thermodynamics of biomembranes. CRC Press, Inc., Boca Raton, Florida.
2. Discher, D. E., D. H. Boal, and S. K. Boey, 1998. Simulations of the erythrocyte cytoskeleton at large deformation. II. Micropipette aspiration. *Biophysical Journal* 75:1584–1597.
3. Fedosov, D. A., B. Caswell, and G. E. Karniadakis, 2010. A multiscale red blood cell model with accurate mechanics, rheology, and dynamics. *Biophysical Journal* 98:2215–2225.
4. Espanol, P., 1998. Fluid particle model. *Physical Review E* 57:2930–2948.
5. Dao, M., J. Li, and S. Suresh, 2006. Molecularly based analysis of deformation of spectrin network and human erythrocyte. *Materials Science and Engineering C* 26:1232–1244.
6. Evans, E., N. Mohandas, and A. Leung, 1984. Static and dynamic rigidities of normal and sickle erythrocytes. Major influence of cell hemoglobin concentration. *The Journal of Clinical Investigation* 73:477–488.
7. Itoh, T., S. Chien, and S. Usami, 1995. Effects of hemoglobin concentration on deformability of individual sickle cells after deoxygenation. *Blood* 85:2245–2253.
8. Helfrich, W., 1973. Elastic properties of lipid bilayers: theory and possible experiments. *Z. Naturforschung C* 28:693–703.